Adıyaman University Journal of Science
https://dergipark.org.tr/en/pub/adyujsci
DergiPark AKADEMİK
ISSN 2147-1630
e-ISSN 2146-586X

Investigation of Structural Properties and Martensitic Phase Transformations in Heat-treated Ni-25.5 at. %Ta High Temperature Shape Memory Alloys

Koksal YILDIZ[1,*]

[1]*Firat University, Faculty of Science, Department of Physics, Elazig, TURKEY*
kyildiz@firat.edu.tr, ORCID: 0000-0002-3484-4653

Received: 08.05.2020 **Accepted:** 04.06.2020 **Published:** 25.06.2020

Abstract

The effect of heat treatment performed at 800 °C, 900 °C and 1000 °C for 1 hour on structural and martensitic transformation properties of Ni-25.5 at.%Ta high temperature shape memory alloy has been examined. Morphological observations by SEM-EDS showed that the heat treatment affected directly microstructural properties of the alloy. Microstructure of the heat treated samples is composed of intermetallic Ni-rich Ni_8Ta and Ta-rich $NiTa_2$ compound in the Ni_3Ta matrix. In addition to these phases, orthorhombic Ni_3Ta phase was only observed in the sample heat-treated at 1000 °C. Structural investigations of alloy the samples by XRD indicated that the martensitic crystal orientation of the samples changed with heat treatments. DSC measurements revealed that all the samples displayed high temperature shape memory behavior with martensitic transformation temperatures of above 200 °C. Vicker's microhardness measurements showed that the microhardness of the alloy influenced dramatically by applying heat treatments, especially at 800 and 900 °C.

Keywords: Ni_3Ta; Martensite; Heat treatment.

* Corresponding Author DOI: 10.37094/adyujsci.733778

Isıl İşlem Uygulanmış Ni-25,5 at. %Ta Yüksek Sıcaklık Şekil Hatırlamalı Alaşımlarındaki Yapısal Özelliklerin ve Martensitik Faz Dönüşümlerinin İncelenmesi

Öz

1 saat boyunca 800 °C, 900 °C ve 1000 °C'de gerçekleştirilen ısıl işlemin, Ni-25,5 at.% Ta yüksek sıcaklık şekil hatırlamalı alaşımının yapısal ve martensitik dönüşüm özellikleri üzerindeki etkisi incelenmiştir. SEM-EDS analizleri ile gerçekleştirilen morfolojik gözlemler, ısıl işlemin alaşımın mikroyapısal özelliklerini doğrudan etkilediğini gösterdi. Isıl işlem uygulanmış numunelerin mikroyapısı, Ni_3Ta anafazı içerisinde dağılmış olan Ni oranınca zengin Ni_8Ta ve Ta oranınca zengin $NiTa_2$ intermetalik bileşiklerinden oluşur. Bu ikincil fazlara ek olarak, ortorombik Ni_3Ta fazı sadece 1000 ºC'de ısıl işleme tabi tutulmuş numunede gözlenmiştir. XRD analizleri ile gerçekleştirilen yapısal analizler, numunelerin martensitik kristal yönelimlerinin ısıl işlemlerle değiştiğini göstermiştir. DSC ölçümleri, tüm numunelerin 200 ºC'nin üzerindeki martensitik dönüşüm sıcaklıkları ile yüksek sıcaklık şekil hatırlama davranışı gösterdiğini ortaya koymuştur. Vickers mikro sertlik ölçümleri, alaşımın mikro sertliğinin özellikle 800 ve 900 ºC'de uygulanan ısıl işlemlerden dramatik bir şekilde etkilendiğini gösterdi.

Anahtar Kelimeler: Ni_3Ta; Martensite; Isıl işlem.

1. Introduction

Shape memory alloys (SMAs) belong to a specific class of smart materials that can remember or retain their previous shape when exposed to thermomechanical or magnetic stimuli. Due to their unique and superior properties, these alloys have become very popular and attracted great interest in many commercial applications in recent years [1, 2]. Binary Ni-Ti alloy is already the most well-known and widely used SMA group and its martensitic transformation temperature is generally below 100 °C. However, at the present time, there is a need for SMAs with higher martensitic transformation temperatures of above 100 °C for high temperature applications, and there are many industrial application areas, at which high temperature SMAs are popular, e.g. sensors and actuators in automotive industry, rocket technologies, nuclear reactor systems and safety devices [3, 4]. Additionally, high-temperature SMAs should have reason for recoverable strain levels, long-term stability, plastic deformation, and adequate environmental resistance [5].

In recent years, binary Ni-Ta alloys, which have high melting temperature and exhibit excellent features in harsh environmental conditions, have attracted attention as a remarkable candidate material, especially for high temperature applications [6]. In 2008, Firstov *et al.* [7] discovered that the intermetallic Ni_3Ta compound also exhibited shape memory behavior with a

martensitic transformation temperature of above 300 ºC. Thus, a new candidate material has been joined in SMA family. The martensitic transformation in intermetallic Ni_3Ta compound occurs resulting in transformation of tetragonal austenite phase to monoclinic martensite phase [8]. The possible phases in the phase diagram of binary Ni-Ta system are liquid solution, Ni-rich fcc-A1, and Ta-rich bcc-A2 solid solutions and intermetallic Ni_8Ta, Ni_3Ta, Ni_2Ta, NiTa and $NiTa_2$ compounds [9, 10]. However, there have been some uncertainties about crystal structures and properties of intermetallic phases in the Ni-Ta system. For example; intermetallic Ni_3Ta is polymorphic with three different crystal structures (orthorhombic *P*mmn-Ni_3Ta, tetragonal *I*4/mmm-Ni_3Ta and monoclinic $P2_1$/m-Ni_3Ta) and which polymorphic phase is stable is still controversial. In addition, the mechanism of the shape memory effect exhibited by the intermetallic Ni_3Ta phase is also unclear [6]. Eventually, it is very important to understand the functional behaviors, such as shape memory effect, and characteristics of intermetallic phases in the binary Ni-Ta system.

The main purpose of this work was to examine the effect of heat treatment performed at 800 °C, 900 °C and 1000 °C for 1 hour on martensitic transformation behavior, morphological and structural properties of high temperature Ni-25.5 at.% Ta SMA were systematically examined by means of DSC, XRD, SEM-EDS and Vicker's microhardness measurements. The effects of heat treatments performed at high temperatures on some physical properties of the non-stoichiometric Ni-Ta SMA, which exhibits shape memory behavior, are studied for the first time.

2. Materials and Methods

The Ni-25.5Ta (at.%) alloy was produced by using high purity nickel (Ni) and tantalum (Ta) powders in an arc-melting furnace under vacuum. The ingot was homogenized at 1400 ºC for 4 hours in a furnace. After the homogenization process, the ingot was cut to different sizes for heat treatments to be performed at different temperatures. The samples were heat treated at 800 ºC, 900 ºC, and 1000 ºC for 1 hour. Sample groups without heat treatment and subjected to heat treatment at 800 ºC, 900 ºC, and 1000 ºC temperatures were labeled as NiTa-0, NiTa-800, NiTa-900 and NiTa-1000, respectively.

Transformation properties of the samples were examined by differential scanning calorimeter (SII NanoTechnology EXSTAR DSC 7000) measurements taken in a nitrogen gas atmosphere at a heating/cooling rate of 10 °C/min. Structural analysis of the samples were realized by taking X-ray diffractometer (Bruker Discover D8 XRD) patterns using Cu K_α radiation at room temperature. Morphological properties and chemical analysis of the samples were studied by carrying out scanning electron microscope (SEM, LEO EVO 40) images equipped with an

energy-dispersive X-ray spectrometer (EDS). The Vicker's microhardness measurements of the samples were performed by using Emco Test DuraScan at a load of 300 g and repeated for five times for each sample.

3. Results and discussion

Fig. 1 displays SEM images of NiTa-0, NiTa-800, NiTa-900 and NiTa-1000 samples. In Fig. 1-a, small-sized gray structures in the matrix of the NiTa-0 sample are clearly visible. From the EDS spectra, it was concluded that the chemical compositions of the matrix and grey structures were composed of 73.69 at.% Ni + 26.31 at.% Ta and 16.97 at.% Ni + 83.03 at.%Ta elements, respectively. According to EDS analyses, it is concluded that this area contains intermetallic Ta-rich $NiTa_2$, which has 1-3 μm in size, sparsely dispersed in the Ni_3Ta matrix. However, Ta content of grey structures in NiTa-0 sample is much higher than that in stoichiometric $NiTa_2$ compound and it is well-known that $NiTa_2$ is only phase with high Ta content in the binary Ni-Ta system. On account of this, it is thought that high Ta content of grey structures in the NiTa-0 sample may be a result of homogenization process. From this, it has been seen that the homogenization condition was not enough to form single phase supersaturated structure. In addition to small-sized Ta-rich $NiTa_2$ precipitate phase in the Ni_3Ta matrix (Fig. 1-a), Ni-rich Ni_8Ta precipitate phases were also observed, containing 83.94 at.% Ni + 16.06 at.% Ta, at different regions of the NiTa-0 sample. Biffi *et al.* [11] detected intermetallic Ni_8Ta and Ni_2Ta precipitates in microstructure of $Ni_{75}Ta_{24}B_1$ alloy homogenized at 1400 ^oC for 4 h. On the other hand, Firstov *et al.* [7] reported that the Ni_8Ta and Ni_2Ta precipitate phases located in the grain boundaries of the Ni_3Ta matrix were disappeared after the same homogenization condition as in Ref. [11]. They did not observe intermetallic $NiTa_2$ compounds in their alloy samples. Eventually, optimal homogenization condition for Ni-Ta alloys are needed to obtain single Ni_3Ta phase structure.

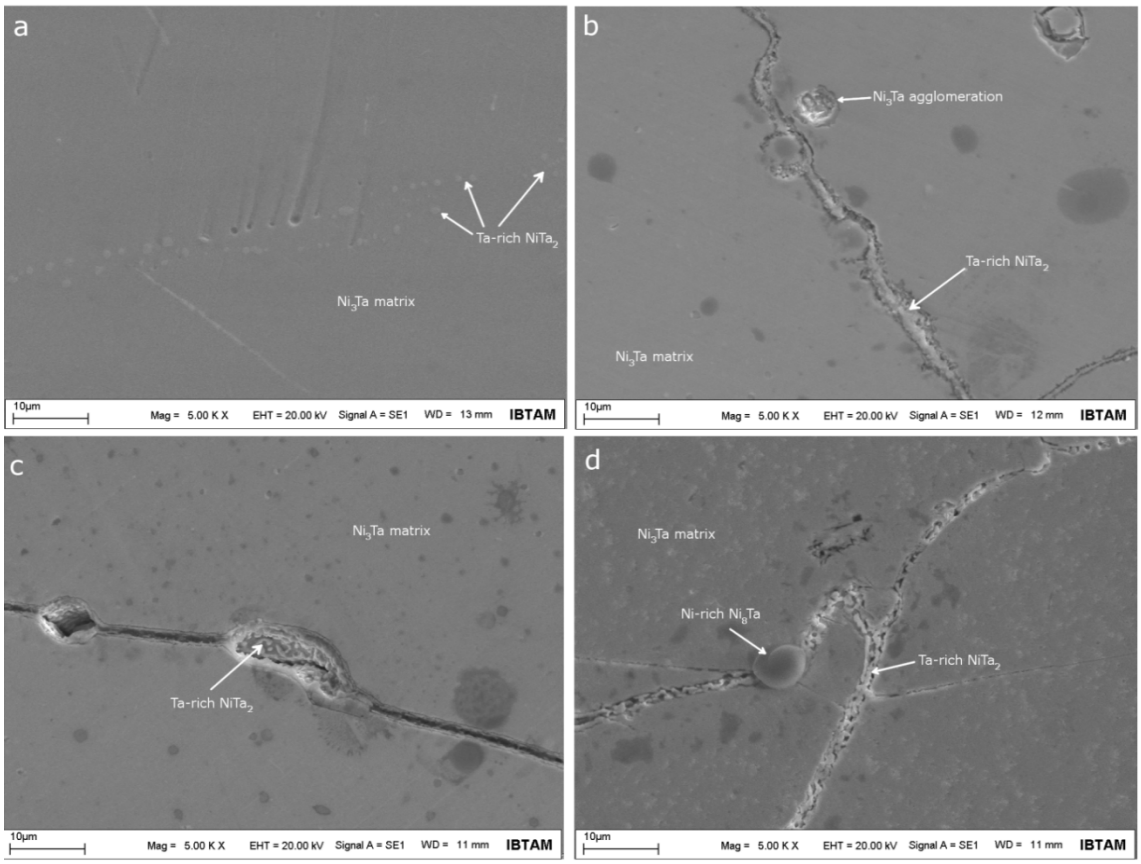

Figure 1: SEM images of (a) NiTa-0, (b) NiTa-800, (c) NiTa-900 and (d) NiTa-1000 alloy samples

The surface morphology of NiTa-800 sample is presented in Fig. 1-b. The heat treatment at 800 ºC led to change in the microstructure of the alloy. The microstructure of NiTa-800 sample contains a large of cracks. Firstov *et al.* [7] reported that intergranular cracks were formed on the surface of Ni_3Ta alloy after homogenization process. However, it could be clearly seen that some secondary phase precipitates in the NiTa-800 sample located in the crack. In order to determine chemical composition of this secondary phase in the crack, point EDS analysis was made. According to EDS analysis, its chemical composition is 30.56 at.% Ni + 69.44 at.% Ta and it is concluded that this phase located in the crack is the Ta-rich $NiTa_2$ phase. From here, it was understood that the Ta-rich $NiTa_2$ phase nucleated and grown in the cracks. Also, in Fig. 1-b, structural agglomerates are observed in some areas of the matrix. According to EDS analysis taken, it was determined that this agglomerate structure in Fig. 1-b chemically included 72.65 at.% Ni + 27.35 at.% Ta elements and this is close to matrix composition. As a result, these agglomerates are not any secondary phases.

SEM image of the NiTa-900 sample is shown in Fig. 1-c. It is obvious that microstructural characteristics of the NiTa-900 sample are similar to that of the NiTa-800. EDS results revealed that the chemical composition of the gray structures in the crack was 20.13 at.% Ni + 79.87 at.%

Ta and these gray structures are the Ta-rich $NiTa_2$ phase as well as observed in NiTa-800 sample. In contrast, the agglomerates observed in NiTa-800 sample disappeared in NiTa-900 sample. In addition, intermetallic Ni_8Ta phase was also detected in some regions of NiTa-900 sample.

Fig. 1-d displays SEM image of the NiTa-1000 sample. Its microstructure contains many cracks and Ta-rich $NiTa_2$ phase (23.76 at.% Ni + 76.24 at.% Ta) located in these cracks. The chemical composition of NiTa-1000 matrix is 74.25 at.% Ni + 25.75 at.% Ta. In addition to these observations, a big-sized structure located on the crack is also visible in Fig. 1-d. Its chemical composition was analyzed by taking EDS spectrum and it is identified as Ni_8Ta phase with 86.68 at.% Ni + 13.32 at%Ta composition. Apart from similar morphological features of NiTa-1000 sample compared to NiTa-800 and NiTa-900 samples, a phase region exhibiting quite different morphological features were also observed in the NiTa-1000 sample. Fig. 2 shows the SEM image of this region. Chemical composition of these structures in Fig. 2 was determined by taking EDS spectra. According to EDS spectra, thin white structures contained 77.2 at.% Ni + 22.8 at.% Ta. From the results of EDS spectra, it is thought that thin white structures are orthorhombic Ni_3Ta phase. Aballe *et al.* [12] showed that prolonged aging process at 800 ºC or above could be caused formation of the stable orthorhombic Ni_3Ta phase in Ni-25wt.% Ta-10wt.% Cr alloy by replacing the b.c.t. Ni_3Ta. Likewise, Kosorukova *et al.* [13] reported that as aging temperature increased the stable orthorhombic Ni_3Ta phase was formed in the Ni_3Ta alloy, as a result of diffusional phase transformation mechanism. Consequently, the results indicated that heat treatment performed at 1000 ºC led to starts diffusional phase transformation in the Ni-25.5Ta (at.%) alloy.

The crack formation in the microstructure of the binary Ni-Ta shape memory alloy is an important issue after homogenization process. It is thought that cracks in the Ni-Ta SMA have a negative effect on its physical properties. Although there are some suggestions to hinder crack formation in the Ni-Ta SMAs [7], Yildiz [14] reported that it might be prevented from the crack formation by changing homogenization condition of Ni-Ta SMA.

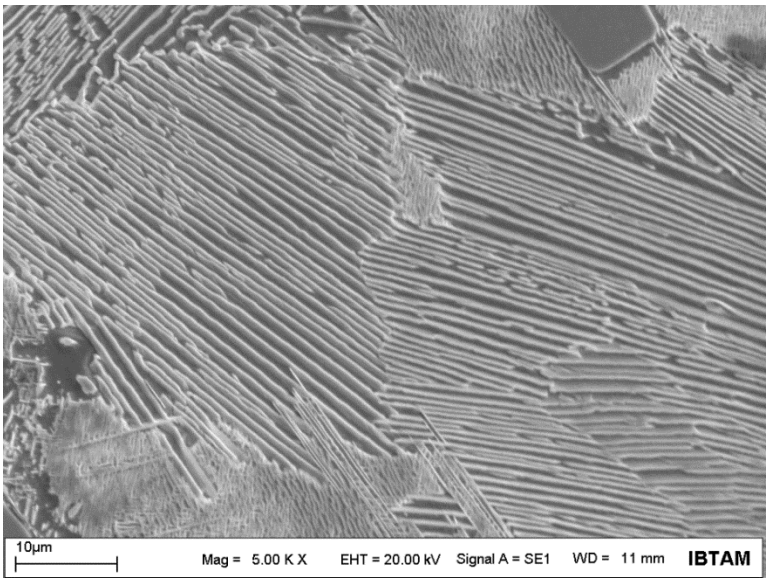

Figure 2: A SEM image showing the stable orthorhombic Ni_3Ta phase in NiTa-1000 sample

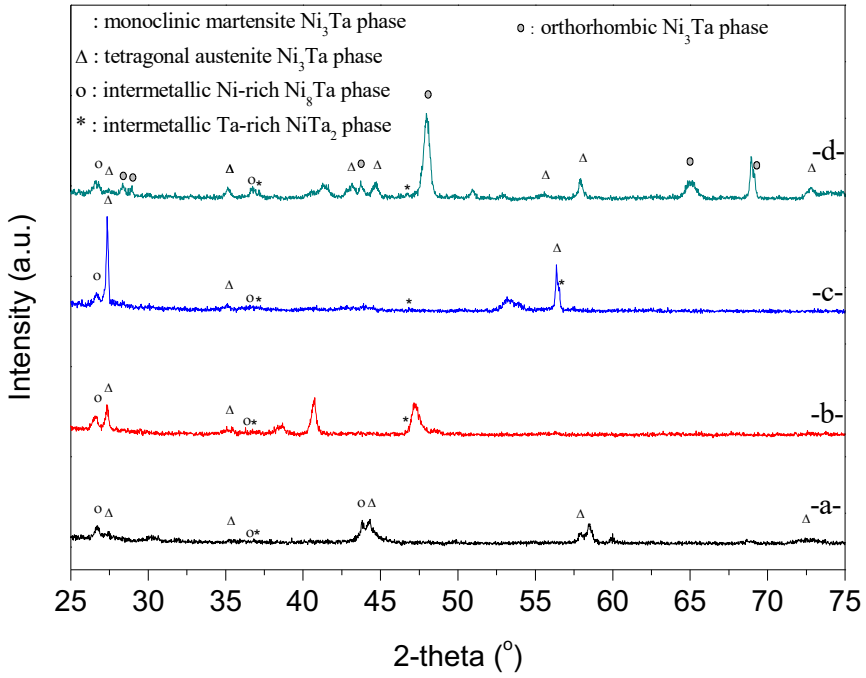

Figure 3: XRD patterns of (a) NiTa-0, (b) NiTa-800, (c) NiTa-900 and (d) NiTa-1000 samples

XRD patterns of NiTa-0, NiTa-800, NiTa-900 and NiTa-1000 samples are illustrated in Fig. 3. The XRD results are in good harmony with the SEM-EDS analysis of the samples. Fig. 3 demonstrates that NiTa-0, NiTa-800 and NiTa-900 samples contain structurally four different phase components: monoclinic martensite Ni_3Ta phase (PDF: 01-073-7070), tetragonal austenite Ni_3Ta phase (PDF: 00-018-0893), and intermetallic Ni_8Ta (PDF: 00-023-0438) and $NiTa_2$ (PDF: 01-072-2592) compounds. However, XRD pattern of NiTa-1000 sample also includes

orthorhombic Ni_3Ta phase (PDF:03-065-2588) in addition to mentioned phases above. The 2θ peak positions of the all phases are also in accordance with the literature [7, 8, 15, 16] and the corresponding phases are marked on patterns. Also, as expected, all samples contained austenite phase at room temperature [11, 13, 17]. The XRD pattern of NiTa-0 sample display in Fig. 3-a. Compared to the XRD patterns in Figs. 3-b and c, it is clear that the heat treatments performed at 800 ºC and 900 °C resulted in significant changes on the crystallographic properties of the alloy. The main martensite phase peak located at $2\theta \approx 43.8^o$ in the XRD pattern of NiTa-0 sample was completely disappeared. However, the peak intensity at $2\theta \approx 27.4^o$, which is quite weak in the XRD pattern of the NiTa-0 sample, increases in the XRD pattern of NiTa-800 sample. As can be seen from the XRD pattern in Fig. 3-c, intensity of this peak is maximum for NiTa-900 sample. These results indicated that the heat treatments at 800 °C and 900 ºC directly affected the martensite phase orientation of alloy. Both number and intensities of the $NiTa_2$ peaks in Fig. 3-c were also increased. This is in good agreement with the SEM observations in Figs. 1-b and c. Finally, from the XRD pattern of NiTa-1000 sample, as shown in Fig. 3-d, it can be clearly seen that the number of related phase peaks increased considerably. The maximum intensity peak in Fig. 3-d is the reflection at $2\theta \approx 47.9^o$ and the diffraction peaks for martensite and orthorhombic phases overlapped. This peak does not exist in the XRD pattern of NiTa-900 sample. The intensity of peak at $2\theta \approx 27.4^o$ in Fig. 3-d is lower than that in the XRD pattern of NiTa-900 sample. Consequently, according to the XRD patterns of all samples in Fig. 3, it is revealed that the crystallographic orientation of martensite phase in the Ni-25.5Ta (at.%) alloy is very sensitive to heat treatments applied at 800 °C, 900 °C, and 1000 °C.

Reverse (martensite to austenite) and forward (austenite to martensite) transformation temperatures of the samples were determined by carrying out DSC scans during heating and cooling curves, as shown in Fig. 4. Austenite start (A_s), austenite finish (A_f), martensite start (M_s) and martensite finish (M_f) temperatures, transformation hysteresis (A_f-M_f) values are tabulated in Table 1. The DSC results in Table 1 indicate that all the samples exhibit high temperature shape memory behavior. It can be also seen that the transformation characteristics of all the samples are well consistent with works in literature [7, 11]. The reverse and forward transformation temperatures were not affected strongly by heat treatment, whereas reverse and forward transformation peak intensities were influenced. The transformation peaks of NiTa-800, NiTa-900 and NiTa-1000 samples are stronger than those of NiTa-0 sample. It is well-known that the heat exchanged during martensitic transformation is related to the amount of martensite phase in the sample [11]. Therefore, it has been concluded that, as a result of heat treatment, the amount of martensite phase in NiTa-800, NiTa-900 and NiTa-1000 samples increased, compared to NiTa-0 sample. This is in a good accordance with the XRD patterns.

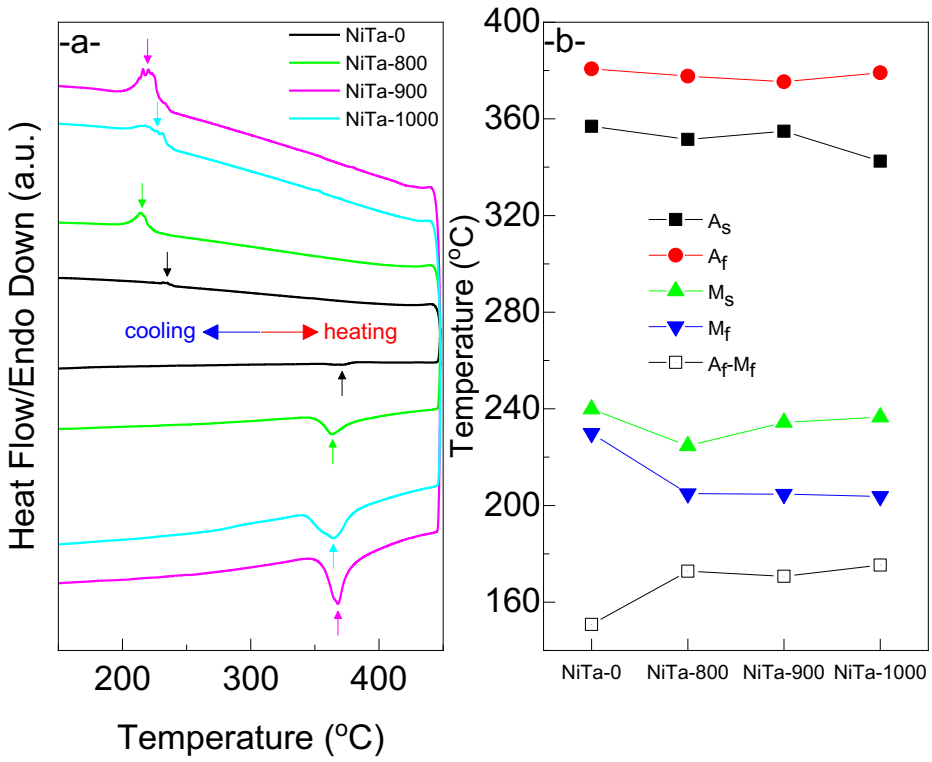

Figure 4: (a) DSC scans of the alloy samples on heating and cooling. (b) Variations of transformation temperatures and hysteresis values of the samples

Table 1: Transformation temperatures and hysteresis values of NiTa-0, NiTa-800, NiTa-900 and NiTa-1000 samples

	A_s(°C)	A_f(°C)	M_s(°C)	M_f(°C)	A_f-M_f(°C)
NiTa-0	356.9	380.7	239.9	229.9	150.8
NiTa-800	351.5	377.7	224.7	204.9	172.8
NiTa-900	354.9	375.4	234.4	204.7	170.7
NiTa-1000	342.5	379.1	236.6	203.8	175.3

Fig. 5 presents variations of the average Vicker's microhardness values of NiTa-0, NiTa-800, NiTa-900 and NiTa-1000 alloy samples. The calculated average Vicker's microhardness values of NiTa-0, NiTa-800, NiTa-900 and NiTa-1000 samples are 460±12, 413.4±7.68, 494.2±13.36 and 460.2±12.96 $Hv_{0.3}$, respectively. The results indicated that heat treatments, especially at 800 and 900 °C, caused a significant change in the microhardness of the alloy.

Another remarkable result is that the average microhardness of NiTa-0 and NiTa-1000 samples are almost the same. Therefore, it has been concluded that the cracks in the microstructure of the alloy samples did not cause significant changes in mechanical behaviors of the samples. However, it is believed that differences in the average microhardness values of NiTa-800 and NiTa-900 samples are closely related to the structural properties of these samples. El Bougory [18] reported that microhardnesses of $Ni_{51}Ti_{49}$ and $Ni_{47}Ti_{49}Co_4$ shape memory alloys altered by the effect of thermal aging and these changes were attributed to change occurring in volume fraction and size of hard precipitates in the microstructures of alloys and also the morphology of martensite plates. Aballe *et al.* [12] noted that heat treatments applied to Ni-Ta-Cr alloys affected the microstructural properties of alloys, resulting in changes in the hardness of alloys. Kojima *et al.* [19] reported that the microhardness of Ni_3Ta compounds subjected to high-energy ion irradiation changed due to changes in lattice structure of the compound.

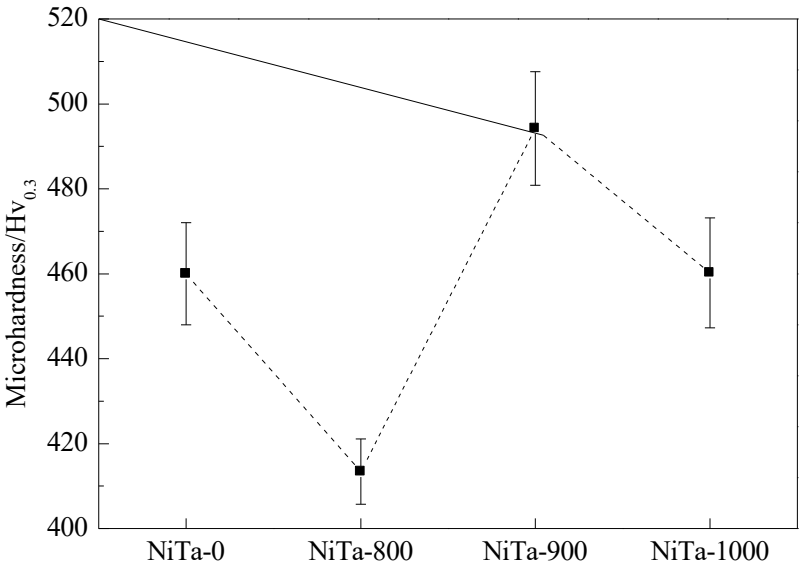

Figure 5: Variation of the average microhardness values of NiTa-0, NiTa-800, NiTa-900 and NiTa-1000 samples

4. Conclusions

Morphological investigations showed that the microstructure of Ni-25.5Ta (at.%) high temperature SMAs changed with applying heat treatment at 800 ºC, 900 ºC, and 1000 ºC. The microstructure of NiTa-0 sample includes intermetallic Ni_8Ta and Ta-rich $NiTa_2$ compounds distributed in Ni_3Ta matrix, whereas the microstructures of NiTa-800, NiTa-900 and NiTa-1000 samples are consisting of Ni_8Ta and Ta-rich $NiTa_2$ compounds and many cracks in Ni_3Ta matrix.

SEM-EDS observations also revealed that the NiTa-1000 sample has the stable orthorhombic Ni_3Ta phase, which is a result of heat treatment at 1000 ^oC. It was observed that volume frictions of intermetallic Ni_8Ta and Ta-rich $NiTa_2$ phases are higher than those of the NiTa-800, NiTa-900 and NiTa-1000 samples. Thermal measurements revealed that all the samples exhibited high temperature shape memory alloy behavior and the heat treatment processes did not affect that. Structural analysis indicated that XRD patterns of all samples were in good consistent with their SEM-EDS observations. The XRD results also demonstrated that the martensitic phase orientation of Ni-25.5Ta (at.%) high temperature SMA was very sensitive to heat treatment. It was deduced that Vicker's microhardness values of the samples changed by applying heat treatment, especially at 800 ^oC and 900 ^oC. This was attributed to change in martensitic phase orientation.

Acknowledgement

This work was supported by Scientific Research Projects Coordination Unit of Firat University under Project number: FF.16.36. The author also thanks to Professor Soner ÖZGEN for his technical support under Project number: FF.15.17.

References

[1] Jani, J.M., Leary, M., Subic, A., Gibson, M.A., *A review of shape memory alloy research, applications and opportunities*, Materials and Design, 56, 1078-1113, 2014.

[2] Taşkan, E., Bulak, S., Taşkan, B., Şaşmaz, M., El Abed, S., El Abed, A., *Nitinol as a suitable anode material for electricity generation in microbial fuel cells*, Bioelectrochemistry, 128, 118-125, 2019.

[3] Rudajevová, A., Pospíšil, J., *Shape memory behavior of a Ni_3Ta alloy pre-deformed in compression*, Materials Science and Engineering A, 527, 2900-2905, 2010.

[4] Wu, K., Ma, J.L., *A review of high-temperature shape memory alloys*, Proceedings of the SMST, p.153, 2000.

[5] Ma, J., Karaman, I., Noebe, R.D., *High temperature shape memory alloys*, International Materials Reviews, 55, 257-315, 2010.

[6] Zhou, Y., Wen, B., Ma, Y., Melnik, R., Liu, X., *First-principles studies of Ni-Ta intermetallic compounds*, Journal of Solid State Chemistry, 187, 211-218, 2012.

[7] Firstov, G.S., Koval, Y.N., Van Humbeeck, J., Ochin, P., *Martensitic transformation and shape memory effect in Ni_3Ta: A novel high-temperature shape memory alloy*, Materials Science and Engineering A, 481-482, 590-593, 2008.

[8] Koval, Y.N., Firstov, G.S., *Nickel-tantalum-New object for investigation of martensitic transformations*, Metallofizika i Noveishie Tekhnologii, 29(6), 815-821, 2007.

[9] Ansara, I., Selleby, M., *Thermodynamic analysis of the Ni-Ta system*, Calphad, 18, 99-107, 1994.

[10] Nash, A., Nash, P., *The Ni-Ta (Nickel-Tantalum) system*, Bulletin of Alloy Phase Diagrams, 5, 259-265, 1984.

[11] Biffi, C.A., Agresti, F., Casati, R., Tuissi, A., *Ni_3Ta high temperature shape memory alloys: effect of B addition on the martensitic transformation and microstructure*, Materials Today: Proceedings, 2S, 813-816, 2015.

[12] Aballe, M., Ramaswamy, V., West, D.R.F., *Intermetallic compound precipitation from solid solution in some Ni-Ta and Ni-Ta-Cr alloys*, Journal of the Less-Common Metals, 39, 287-292, 1975.

[13] Kosorukova, T., Firstov, G., Noël, H., Ivanchenko, V., *Crystal structure changes in the Ni_3Ta intermetallic compound*, Chemistry of Metals and Alloys, 6, 196-199, 2013.

[14] Yildiz, K., *Thermally induced martensitic transformation and structural properties in Ni-Ta high-temperature shape memory alloys*, The European Physical Journal Plus, 134, 11, 2019.

[15] Larson, J.M., Taggart, R., Polonis, D.H., *Ni_8Ta in nickel-rich Ni-Ta alloys*, Metallurgical and Materials Transactions B, 1, 485-489, 1970.

[16] Kripyakevich, P.I., Pylaeva, E.N., *Crystal structure of the compound Ta_2Ni*, Journal of Structural Chemistry, 3, 30-32, 1962.

[17] Kosorukova, T.A., Firstov, G.S., Koval, Y.N. Van Humbeeck, J., Zhuravlev, B., *Phase transformations and shape memory behavior in Ni_3Ta-based intermetallics*, Materials Today: Proceedings 2S, 793-796, 2015.

[18] El-Bagoury, N., *Comparative study on microstructure and martensitic transformation of aged Ni-rich NiTi and NiTiCo shape memory alloys*, Metals and Materials International, 22, 468-473, 2016.

[19] Kojima, H., Yoshizaki, H., Kaneno, Y., Semboshi, S., Hori, F., Saitoh, Y., Okamoto, Y., Iwase, A., *Lattice structure transformation and change in surface hardness of Ni_3Nb and Ni_3Ta intermetallic compounds induced by energetic ion beam irradiation*, Nuclear Instruments and Methods in Physics Research Section B, 372, 72-77, 2016.